IOP Publishing Journal of Optics A: Pure and Applied Optics
J. Opt. A: Pure Appl. Opt. **9** (2007) 239–242 doi:10.1088/1464-4258/9/3/005

A plain photonic crystal for generating directional radiation from embedded sources

K Guven[1,2] **and E Ozbay**[1,2,3]

[1] Nanotechnology Research Center, Bilkent University, 06800 Ankara, Turkey
[2] Department of Physics, Bilkent University, 06800 Ankara, Turkey
[3] Department of Electrical and Electronics Engineering, Bilkent University, 06800 Ankara, Turkey

Received 9 May 2006, accepted for publication 11 January 2007
Published 2 February 2007
Online at stacks.iop.org/JOptA/9/239

Abstract
We investigate experimentally the generation of highly directional radiation from a plain two-dimensional photonic crystal structure where an embedded source couples to a photonic crystal band having Bloch modes of even symmetry and negative group velocity. No modification is made to the crystal structure. By virtue of recent studies employing corrugated surface modes, this may be a viable method for generating directional radiation for antenna applications.

Keywords: photonic crystal, directional radiation, negative refraction

(Some figures in this article are in colour only in the electronic version)

1. Introduction

The utilization of photonic crystals (PCs) for controlling the enhancement (or inhibition), and the spatial confinement, of the electromagnetic radiation of luminescent sources has been an active research area since the beginning of the recognition of PCs as novel photonic tools [1]. Different aspects of this subject were investigated and reported in the literature; part of these studies utilize the PC as a cover or substrate to the externally located source [2–6]. Other studies consider embedded sources [7–11] where the PCs are employed in several ways to achieve enhanced and highly directional radiation. The enhancement of the radiation can be obtained by constructing a PC which has a bandgap at the emission frequency of the source, thereby suppressing the radiation loss through propagating modes. The radiation is then extracted by coupling the source to a coupled cavity waveguide mode [5], or a grating coupler [6]. However, the extracted emission does not necessarily have a spatial confinement, unless the waveguide exit is corrugated to support surface modes which can induce a directional beam [12, 13]. Another approach is coupling the source preferentially to the propagating modes, which are governed by a flat dispersion in certain directions. This results in the so-called 'self-guiding modes' of the photonic crystal [14, 15]. This phenomenon stems from the anisotropy of the band structure of the PC and does not require a full bandgap or a dielectric boundary to spatially confine the propagating modes.

Enoch *et al* performed an extensive theoretical analysis of the spatial control of the electromagnetic field propagating within the PC and emitted from the PC based on the band structure [8, 9]. In particular, they have shown by simulations that a directional beam from an embedded source can be obtained by using a hexagonal PC which is expanded in a certain crystal direction (ΓK). Further, one emitting surface of the expanded PC can be covered with a similar but unexpanded PC to block the radiation so that the resulting structure generates a directional beam only from one surface [8]. A number of experiments are reported which investigated [16] and utilized [10] the photonic band edges for directional emission.

In this paper, we report an experimental and numerical study of the directional radiation from a uniform PC structure with an embedded source. Our main motivation is to demonstrate that, complementary to the studies mentioned above, it is possible to generate a highly directional beam from a plain two-dimensional bulk photonic crystal without any modification in terms of its geometrical and material parameters. Employing a photonic band with appropriate topology suffices to channel the radiation of the embedded

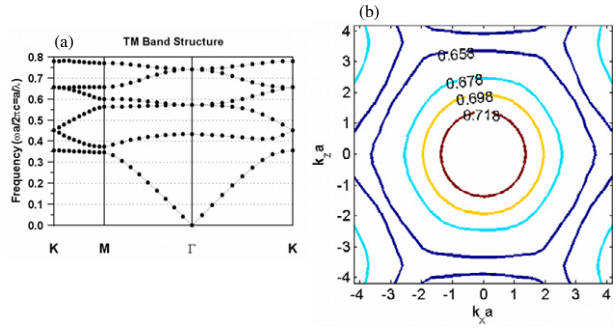

Figure 1. (a) The first six TM polarized bands of the 2D PC plotted in the Brillouin zone. The fifth band is utilized for the directional radiation. (b) Several equal-frequency contours (EFC) of the fifth band in the full Brillouin zone. The contours shrink with increasing frequency.

source and then transfer it to free space in the form of a directional beam. In addition, strong isolation of the emitted radiation in the lateral direction is achieved within a compact sized crystal. The beam exits the radiating surface with very narrow spatial extent. In this study, we consider the planar confinement of the radiation only. Out-of-plane losses—which are evidently significant for a finite size PC—are not taken into account. One method of reducing the out-of-plane losses is to use additional PC covers at both ends of the relevant bulk PC which block the propagation in the transverse direction. Obviously, using a 3D PC with a band structure similar to that investigated here can provide better isolation in the lateral and transversal directions.

We used a transverse magnetic polarized band of the 2D PC. The convention is taken such that the magnetic field vector is parallel to the rods of the PC (the electric field is in the plane of propagation). To our knowledge, the directional beam experiments using photonic crystals reported so far considered the transverse electric polarization only.

2. Band structure analysis of the photonic crystal

The photonic crystal used in this study is a 2D hexagonal array of cylindrical alumina rods. The rods are 150 mm long, have a radius of 1.55 mm and a dielectric constant of $\varepsilon = 9.61$. In the simulations, the PC is invariant in the direction of the rods. The period of the crystal, a, is set to be 4.794 mm.

We start by analysing the band structure which is the underlying mechanism for shaping the radiation pattern. A commercially available band structure solver (Bandsolve) is used to obtain the band structure for a periodic PC. This provides a fairly good approximation for finite-size PCs, unless very small crystal sizes are of concern. Figure 1(a) shows the first six TM polarized bands of the PC calculated by the plane-wave expansion method. For obtaining directional radiation, the fifth band will be utilized.

Several equal-frequency contours (EFC) close to the lower edge of the fifth band are plotted in figure 1(b). Close to the band edge, the contours conform to the Brillouin zone (hexagonal shape) with nearly flat edges normal to the ΓM direction. It has been shown that the Bloch modes within the PC possess even symmetry when the wavevector, $\boldsymbol{k}$, is along the ΓM direction, and odd symmetry when $\boldsymbol{k}$ is along the ΓK direction, whereas a plane wave propagating in free space at normal incidence is of even symmetry [17]. When a PC surface is normal to the ΓM direction, the Bloch modes with matching symmetry can couple to free space with very high transmission. In loose terms, one may say that a 'properly cut' PC emits radiation only along certain crystal directions. This property will be illustrated further below.

The self-guiding [14] and self-focusing [15] of the Bloch modes within the 2D photonic crystals were investigated theoretically and reported extensively in the literature. The photonic band we employ here meets the condition for the spatial confinement of the propagation within the PC, namely by the flat dispersion at its low frequency edge. Since the directivity is achieved through the refraction of the beam at the PC–free-space interface, an effective index of refraction, n_{eff}, can be introduced to characterize the refractive properties for the particular frequency band. For a photonic crystal, n_{eff} is defined as $n_{\mathrm{eff}} = \mathrm{sgn}(\vec{v}_{\mathrm{g}} \cdot \vec{k}_{\mathrm{f}})(c|\vec{k}_{\mathrm{f}}|/\omega)$, where $\vec{v}_{\mathrm{g}} = \vec{\nabla}_k \omega$ is the group velocity and $\vec{k}_{\mathrm{f}}$ is the wavevector inside the PC [18–20]. When the EFCs are convex (i.e. shrinking with increasing frequency as in figure 1(b)) the group velocity and the phase velocity $\vec{v}_{\mathrm{p}} = (c/|n_{\mathrm{p}}|)\hat{k}_{\mathrm{f}}$ are antiparallel and the associated n_{eff} becomes negative (here, n_{eff} and n_{p} are identical). Evidently, n_{eff} is anisotropic both in frequency and wavevector, by virtue of the topology of the EFCs. It should be emphasized that the n_{eff} obtained here does not imply a homogeneous medium which can replace the photonic crystal. We use n_{eff} only to describe the refractive properties within this particular band. Similarly, a n_{eff} extracted from Snell's law is only descriptive for the refraction properties. Here, we consider the Snell's law only to illustrate that at the PC–air interface ($n_{\mathrm{eff}} \sin\theta_{\mathrm{PC}} = n_{\mathrm{air}} \sin\theta_{\mathrm{air}}$), θ_{air} will be a small quantity when $n_{\mathrm{eff}} \ll 1$. If n_{eff} is both small and *negative*, the directivity may improve further as this induces a slight focusing of the beam as it propagates away from the PC interface.

3. Measurements and simulations

Based on this analysis, we set up an experiment to measure the radiation pattern of a PC with an embedded source. We also simulated the experimental structure by the finite difference time domain (FDTD) technique, using commercial software (RSoft Fullwave). The simulation is performed in 2D. The PC has 17 layers along the x (ΓK) direction and 13 layers along the y (ΓM) direction. A point source is located at the centre of the PC, where a dielectric rod is removed. The computational structure is normalized to have a PC period of unit value. The spatial grid step is 0.05 in x and y directions. A stable time step of 0.0312 is used. Figure 2(a) shows the two-dimensional pattern of the squared electric field, $|E(x, y)|^2$, at $\omega = 0.67$ ($f = 41.9$ GHz) computed by FDTD simulation. The strong directionality of the radiation along the ΓM direction, and the suppression of radiation in the ΓK direction, are clearly observed in this simulation. In figure 2(b), the corresponding experimental pattern is plotted. The measurement is performed by a 2D spatial scanning set-up and two probe antennas, one inserted into the PC and the other mounted on the scanning probe. The transmission spectrum is measured by a network analyser. The calibration measurement is taken in the absence

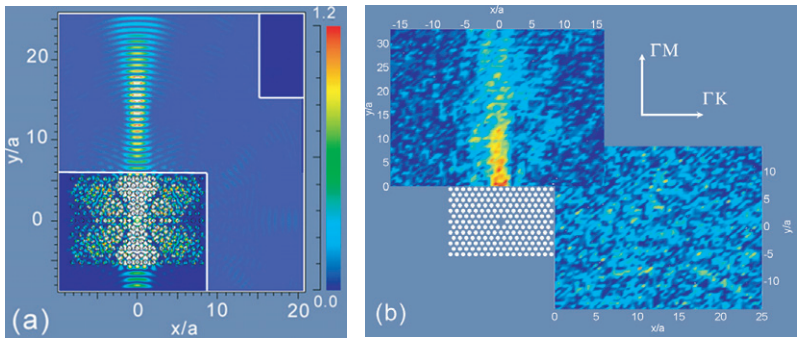

Figure 2. (a) Simulated electric field-squared pattern of a source with $f = 41.9$ GHz located at the centre of the PC over a rectangular area. The PC is a 17×13 layer rectangular slab. The light shaded area corresponds roughly to the experimentally scanned region. (b) The experimental field-squared pattern obtained by scanning two rectangular regions along the ΓM (x) and ΓK (y) directions, respectively.

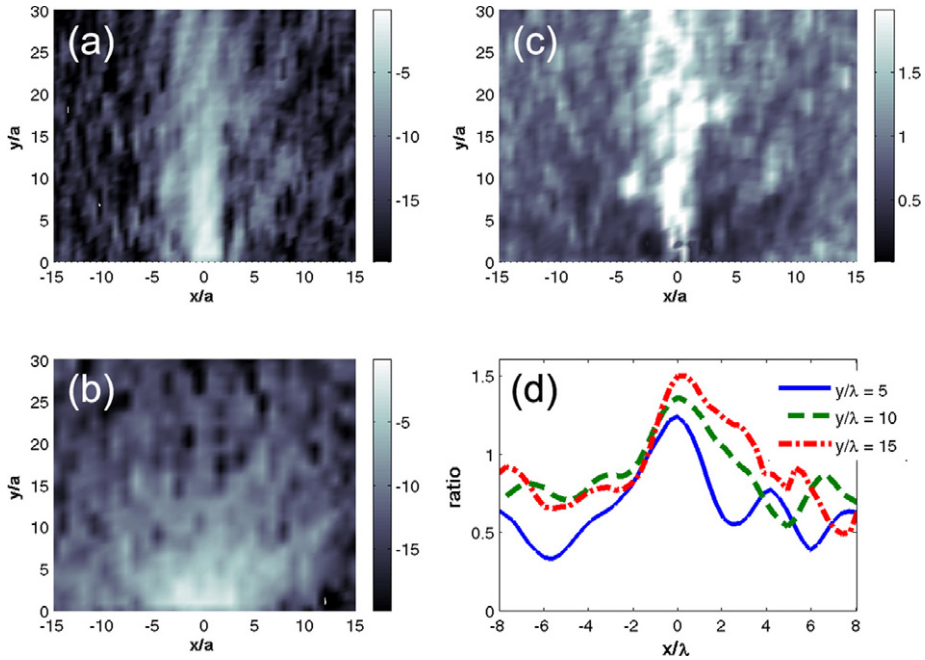

Figure 3. (a) The experimental $|E(x, y)|^2$ map along the ΓM direction starting from the PC surface for an embedded source radiating at $f = 41.9$ GHz. The intensity is measured in the dB scale. (b) Same as in (a), in the absence of the photonic crystal. (c) The ratio of the maps depicted in (a) and (b). (d) The lateral beam profiles at locations $y/\lambda = 5$, 10 and 15 taken from the map in (c). A value greater than 1 indicates enhancement with respect to free space.

of the PC, the scanning probe being located at $x = 0$ and at the y coordinate which corresponds to the location of the PC surface.

The experimental map in figure 2(b) is combined from two separate measurements, each performed on a rectangular area in the ΓM and ΓK directions, respectively. The axes are scaled by the PC period. The intensity scale of the experimental plot ranges from 0 dB to 1.2 linearly. The directional beam emerging from the ΓM surface is clearly observable. The measurements are not taken in an anechoic chamber, therefore some background is present.

In figure 3, we compare the map of $|E(x, y)|^2$ obtained in the (a) presence and (b) absence (i.e. free space) of the photonic crystal. Figure 3(c) shows the free-space normalized map (the ratio of (a) and (b)). In figure 3(d) the lateral profiles of the free-space normalized map at locations $y/\lambda = 5$, 10 and 15 (relative to the PC surface) are plotted. We conclude that the radiation along the propagation axis is enhanced (values greater than unity), whereas the lateral spread is suppressed (values less than unity). The FHWM is on a par with few wavelengths, but still remains confined throughout the propagation up to the measured range.

Figure 4 depicts a simulation of a cubic-cut and a hexagonal-cut PC. This shows that, when the PC surface geometry mimics the Brillouin zone edges, the radiation is effectively transmitted to free space, since all surfaces are perpendicular to the ΓM direction. The square-cut PC still provides a directional beam, but in this case, noticeable side-lobes are present along the diagonal directions. A rectangular geometry with a higher aspect ratio in the lateral direction isolates the ΓK surfaces better.

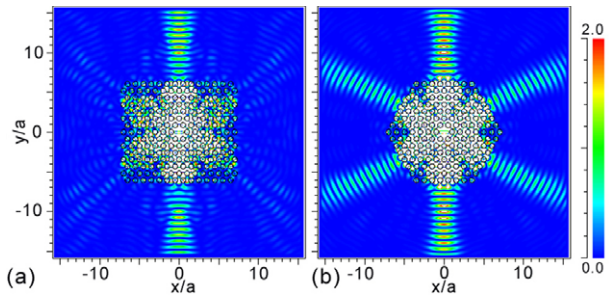

Figure 4. The radiation intensity pattern for (a) cubic- and (b) hexagonal-cut photonic crystals. The source radiates at $f = 41.9$ GHz.

4. Conclusion

In summary, we have investigated the angular confinement of the radiation from a luminescent source embedded in a bulk PC structure. The presence of directional radiation in a certain spatial direction is demonstrated experimentally and by simulations. The lateral beam profile is observed to be confined for a distance up to 15λ away from the radiating surface of the photonic crystal. The confinement is the combined effect of the coupled photonic band with appropriate dispersion and of the surface geometry of the PC. This type of photonic crystal may be useful for certain antenna applications or in future integrated microwave photonic circuits requiring narrow beam profiles.

Acknowledgments

This work is supported by the European Union under the projects EU-NoE-METAMORPHOSE, EU-NoE-PHOREMOST and TUBITAK under Projects No. 104E090, 105E066, 105A005 and 106A017. One of the authors (EO) also acknowledges partial support from the Turkish Academy of Sciences.

References

[1] Yablonovitch E 1987 *Phys. Rev. Lett.* **58** 2059
[2] Qiu M and He S 2001 *Microw. Opt. Technol. Lett.* **30** 41
[3] Gonzalo R, de Maagt P and Sorolla M 1999 *IEEE Trans. Microw. Theory Tech.* **47** 2131
[4] Kesler M P, Maloney J G, Shirley B L and Smith G S 1996 *Microw. Opt. Technol. Lett.* **11** 169
[5] Bayindir M, Tanriseven S, Aydinli A and Ozbay E 2001 *Appl. Phys.* A **73** 125
[6] Fehrembach A L, Enoch S and Sentenac A 2001 *Appl. Phys. Lett.* **79** 4280
[7] Biswas R, Ozbay E, Temelkuran B, Bayindir M, Sigalas M M and Ho K-M 2001 *J. Opt. Soc. Am.* B **18** 1684
[8] Enoch S, Gralak B and Tayeb G 2002 *Appl. Phys. Lett.* **81** 1588
Enoch S, Tayeb G and Gralak B 2003 *IEEE Trans. Antennas Propag.* **51** 2659
[9] Enoch S, Tayeb G, Sabouroux P, Guérin N and Vincent P 2002 *Phys. Rev. Lett.* **89** 213902
[10] Bulu I, Caglayan H and Ozbay E 2003 *Appl. Phys. Lett.* **83** 3263
[11] Kramper P, Agio M, Soukoulis C M, Birner A, Müller F, Wehrspohn R B, Gösele U and Sandoghar V 2004 *Phys. Rev. Lett.* **92** 113903
[12] Bulu I, Caglayan H and Ozbay E 2005 *Opt. Lett.* **30** 3078
[13] Kosaka H, Kawashima T, Tomita A, Notomi M, Tamamura T, Sato T and Kawakami S 1999 *Appl. Phys. Lett.* **74** 1212
[14] Chigrin D N, Enoch S, Torres C M S and Tayeb G 2003 *Opt. Exp.* **11** 1203
[15] Martinez A, Miguez H, Griol A and Marti J 2004 *Phys. Rev.* B **69** 165119
[16] Koenderink A F and Vos W L 2003 *Phys. Rev. Lett.* **91** 213902
[17] Ruan Z C, Qiu M, Xiao S S, He S L and Thylén L 2005 *Phys. Rev.* B **71** 045111
[18] Foteinopoulou S, Economou E N and Soukoulis C M 2003 *Phys. Rev. Lett.* **90** 107402
[19] Foteinopoulou S and Soukoulis C M 2003 *Phys. Rev.* B **67** 235107
[20] Parimi P V, Lu W T, Vodo P, Sokoloff J, Derov J S and Sridhar S 2004 *Phys. Rev. Lett.* **92** 127401